Comparison and Combination of Iris Matchers for Reliable Personal Identification

Ajay Kumar, Arun Passi
Biometrics Research Laboratory
Department of Electrical Engineering, Indian Institute of Technology Delhi
Hauz Khas, New Delhi 110 016, INDIA

Abstract

The biometric identification approaches using iris images are receiving increasing attention in the literature. Several methods for the automated iris identification have been presented in the literature and those based on the phase encoding of texture information are suggested to be the most promising. However, there has not been any attempt to combine these phase preserving approaches to achieve further improvement in the performance. This paper presents a comparative study of the performance from the iris identification using log-Gabor, Haar wavelet, DCT and FFT based features. Our experimental results suggest that the performance from the Haar wavelet and log Gabor filter based phase encoding is the most promising among all the four approaches considered in this work. Therefore the combination of these two matchers is most promising, both in terms of performance and the computational complexity. Our experimental results from the all 411 users (CASIA v3) and 224 users (IITD v1) database illustrate significant improvement in the performance that is not possible with either of these approaches individually.

1. Introduction

The iris identification has emerged as a preferred modality for the large-scale user authentication and has significantly higher user-acceptance as compared to the retinal identification, which is generally believed to be more reliable. The iris patterns are highly stable and unique as the probability for the existence of two irises that are same has been estimated to be very high, *i.e.* one in 10^{72} [8]. The iris is the colored annular ring whose size is controlled by the biological tissues while adjusting the amount of light entering the pupil. With its stripes, pits and furrows the iris offers numerous individual attributes which are distinct even between the identical twins and between the left and right eyes of a person.

1.2 Related Work and Motivation

The iris identification using analysis of the iris texture has attracted lot of attention and researchers have presented variety of approaches in the literature [1]-[10]. Daugman [2] has presented most promising 2D Gabor filter based approach for the iris identification system that employed 2048 bit iris-code. Boles [5] has detailed fine-to-coarse approximation at different resolution levels that are based on zero-crossing representation from the wavelet transform decomposition. Wildes *et al*. [7] have focused on efficient implementation of gradient-based iris segmentation using Laplacian pyramid. Proença and Alexandre [8] have suggested region-based feature extraction for the iris images acquired from large distances. Thornton *et al*. [1] have recently estimated the non-linear deformations from the iris patterns and proposed a Bayesian approach for reliable performance improvement. Huang *et al*. [10] have demonstrated the usage of phase-based local correlations for matching iris patterns and achieved notable performance over the prior techniques. Li Ma *et al.* [4], [6] employed multi-scale bandpass decomposition and evaluated comparative performance from prior approaches.

The summary of prior work [17] suggests that there have been very little efforts to combine the promising approaches presented in the literature and investigate the performance improvement. It may be noted that such combination should have merit of improved accuracy and requires relative performance analysis of for the candidate approaches. It is generally believed that the acquisition of large number registration/training images cause inconvenience to the users and therefore smaller number of training images is always desirable. Therefore the performances from the prior approaches, or from the proposed combination, need to be evaluated using minimum[†] training set to ascertain its effectiveness.

2. Our Work

The work detailed in this paper focuses on the comparative performance evaluation from the phase encoding of iris patterns using four approaches; Haar wavelet, Gabor filter, Discrete Cosine Transform (DCT), and Fast Fourier Transform (FFT) based feature extraction. The resulting combination of the best performing approaches is used to investigate the further performance improvement. The experimental results illustrated in this paper suggest that the performance from the Haar wavelet and log Gabor filter based phase encoding is the most promising among all the four approaches considered in this work. Therefore the simultaneously extracted matching scores from these two matchers are combined for further performance improvement.

Our implementation of the considered four approaches is largely based on their details presented in the literature. While evaluating these approaches, various combinations of parameters are attempted, separately for

[†] The minimum or one training image performance is of significant interest in the forensic analysis.

three different databases, to achieve the best possible performance. In the following subsections, we briefly describe these matchers and our implementation for the comparative performance evaluation.

2.1 Discrete Cosine Transform

The iris recognition using the phase information from the zero crossings of the one dimensional DCT has shown promising result in [3]. The DCT coefficients $C(u)$ from the signal $f(x)$ of length L are obtained as follows:

$$C(u) = \varepsilon(u) \sum_{x=o}^{L-1} f(x) \cos\left[\frac{\pi . u}{2.L}(2x+1)\right], \quad \forall\, u = 0, 1, ..., L-1 \quad (1)$$

where $\varepsilon(u) = \frac{2}{L}$ for $u \neq 0$ and $\varepsilon(u) = \frac{2\sqrt{2}}{L}$ for $u = 0$. Our implementation of this approach was iteratively tuned to achieve the best performance. The skewing of successive rows by one pixel to the right was used to extract the blocks orientated at 45°. Then the weighted average under a 1/4th Hanning window is performed on each block which reduces the horizontal resolution and the degrading effects of noise and generates a 1D vector. That vector is then windowed using a similar Hanning window in the vertical direction before the application of DCT. Now, difference of adjacent DCT output vectors are calculated and feature vector is formed from their zero crossings. The size of the feature vector depends on the amount of information (bits) retained after the application of DCT. For matching of two iris templates a modified version of hamming distance is used in which the product of sum of respective bits corresponding to each block as detailed in [3]:

$$S = \left(\prod_{i=1}^{M} \frac{\sum_{j=1}^{N} Block1_{ij} \oplus Block2_{ij}}{N} \right)^{1/M} \quad (2)$$

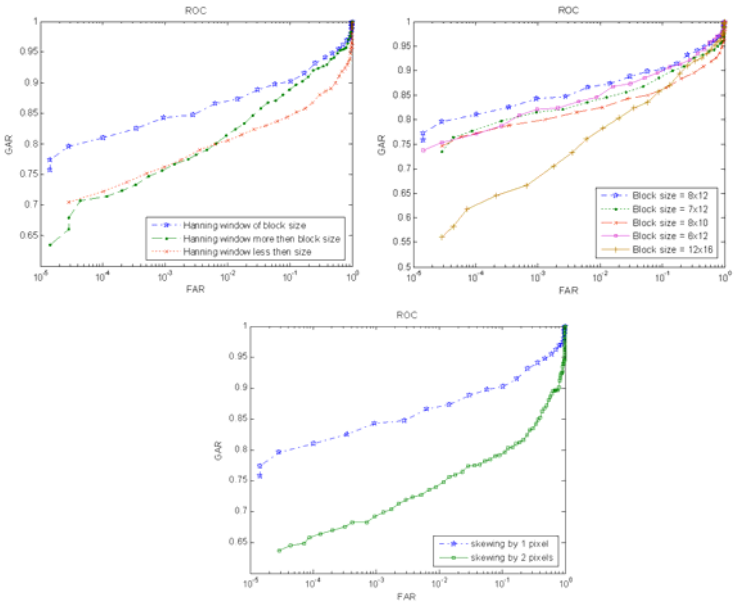

Figure 1: Selection of block size and their orientation for DCT features using one training image

where, M is the number of bits per block in vertical direction, N is the total number of blocks. The figure 1 illustrates the selection of block size and their orientation, (skew) from the achieved performance, when only one image was used for the training and rest six images are used for evaluation.

2.2 Fast Fourier Transform

The local frequency variations can also be employed for encoding the phase information from the iris texture. The enhanced iris images are firstly divided into block aligned at 45°. The blocks are then averaged in the horizontal direction and then multiplied by a Hanning window, which results in a 1D signal corresponding to each block. This signal $f(x)$ is employed to extract the one dimensional FFT coefficients, $F(k)$, as follows:

$$F(k) = \sum_{x=1}^{L} f(x) \exp\left\{\frac{-2\pi j(k-1)}{L}\right\}, \quad \forall\, k = 1, 2 ..., L \quad (3)$$

The difference in the magnitude of adjacent blocks is computed and a binary feature vector is formed from the zero crossings of each difference. The size of the blocks was chosen to be 8 × 12 with an overlapping of 4 pixels in the vertical direction and 6 pixels in the horizontal direction. The size of the resulting feature vector was 8160 bits and Hamming distance was used to measure the difference between the feature vectors.

2.3 Haar Wavelet

The feature extraction using the four level Haar wavelet decomposition of the enhanced image was firstly investigated. The diagonal coefficients of the fourth level were employed to obtain 4 × 32 real values. In addition to these 128 values, the average of diagonal coefficients from the first, second and third level decomposition were also employed. Each of those 131 (3 + 128) values were quantized to binary values by simply converting the positive values to 1 and negative values to 0. Therefore, the feature vector for any iris constituted of only 131 bits. The Hamming distance was again employed to match two feature vectors. However, as shown in figure 2, the performance from these features was poor and therefore we also investigated higher level wavelet coefficients.

In this approach, the enhanced images are decomposed into 5 levels by the Haar wavelets [11]. Next the vertical, horizontal and diagonal coefficients of 4th and 5th level were employed. The coefficients of 1st, 2nd, and 3rd level were almost the same as those of the 4th level and therefore the smallest of them (4th level coefficients) were employed and rest were ignored. The 5th level decomposition offered the most discriminative information and therefore all the coefficients from this decomposition were employed. The phase encoding from the zero crossings of the coefficients formed the binary values of the feature vector. The size of this feature vector was 3 times the size of features of 4th level (4 × 32) plus 3 times the features of 5th

level (2 × 16), therefore in total the size of feature vector was 480 bits. The Hamming distance was then employed to ascertain the matching distance between feature vectors. The shifting of feature vectors to the left and right by 12 bits can account for the possible rotation of the extracted iris and significantly improved the performance as shown in figure 2 (one training image and seven test images per user).

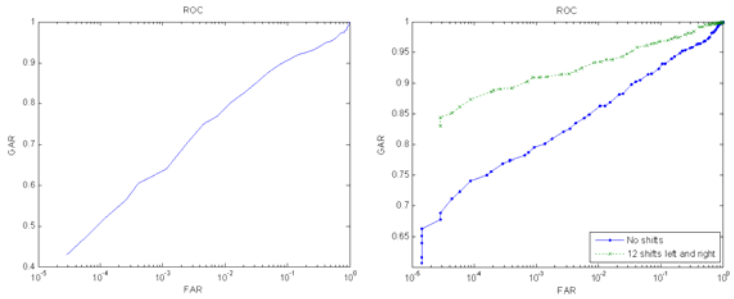

(a) (b)

Figure 2: The performance from the Haar wavelet based approach using 4 in (a) and 5-level decomposition in (b)

2.4 Log-Gabor Filter

The features extracted from the phase encoding of iris texture have gained lot of attention since the fundamental work of Daugman [2]. The Gabor filters over represent the low frequency components and under represent the high frequency components in any encoding and an even-symmetric Gabor filter will have a DC component whenever the bandwidth is larger than one octave. Therefore the Log-Gabor filters have been recently suggested [12]-[13] for phase encoding because the zero DC-component can be obtained for any bandwidth by using a Gabor filter which is Gaussian on a logarithmic scale. The Log-Gabor filters having extended tails at the high frequency end are expected to offer more efficient encoding of natural images [14].

The Log-Gabor function has singularity in the log function at the origin, therefore the analytic expression for the shape of the Log-Gabor filter cannot be constructed in spatial domain. Therefore the filter is implemented in frequency domain The frequency response of Log-Gabor filter in frequency domain is defined as follows:

$$G(f) = \exp\left(\frac{-(\log(f/f_o))^2}{2(\log(\sigma_f/f_o))^2}\right) \quad (4)$$

with f_0 is the central frequency and σ_f is the scaling factor of the radial bandwidth B. The radial bandwidth in octaves is expressed as follows:

$$B = 2\sqrt{2/\ln 2} * \left|\ln(\sigma_f / f_0)\right| \quad (5)$$

The parameters for the Log-Gabor filter performance were empirically selected to achieve the best performance; the center wavelength of 18 and the ratio σ_f / f_0 of 0.55 achieves the best performance and was therefore employed for CASIA I database. Similarly the center wavelength of 22 and σ_f / f_0 equal to 0.55 can achieve best performance for CASIA III database and was therefore selected for the entire performance evaluation reported in this paper. The minimum of the Hamming distance from the 12 comparisons (template shifts) is used as the final matching distance.

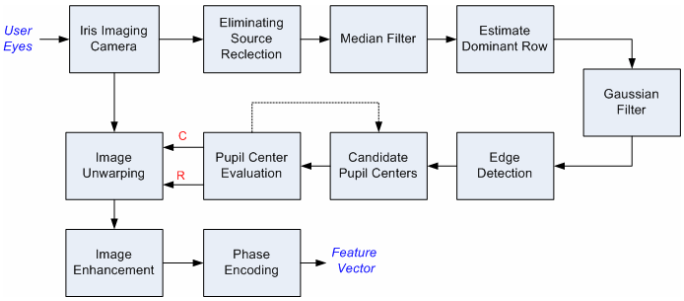

Figure 3: The image normalization steps for extracting iris.

3. Preprocessing and Normalization

The entire steps for the extraction of normalized iris regions from the acquired images were iteratively refined and implemented efficiently for online identification. The pupil in the acquired image usually contains reflection from the illumination source, which forms some bright spots in the pupil, so if the pixel value inside the pupil is over a particular threshold (200) then it is replaced by pixel value of some neighborhood pixel. This operation almost fills the circles but this still it is not good enough to apply a global threshold for the pupil circle estimation. Therefore the image is passed through a 7 × 7 median filter (figure 3).

The pupil is usually very distinct black circle, the pupil center in our approach is estimated by scanning the image row-wise and number of consecutive pixels whose value is less than certain threshold (say 65 in our implementation), are calculated for every row. The row containing the highest number of such consecutive pixels must correspond to the diameter of the pupil, half of that maximum value corresponds to the radius of the pupil, the *y* coordinate of the center of pupil is the row of the diameter and the *x* coordinate is calculated by adding radius of pupil to the column from where the consecutive pixels started.

The contrast from the image filtered from the median filter is higher and therefore its subjected to the Gaussian filtering to remove further noise due to iris texture, then the edge detection is performed using the canny edge detector.

After the edge detection a 20 × 20 window is chosen in the edge detected image around the center of the pupil. Then every pixel in this window is assumed as the center (candidate centers) and the numbers of white pixels, that are encountered at the perimeter of circle, with radius varying from 80 to 120 pixels, are computed. The winner, *i.e.*, the radius (among 80-120 pixel) and the center (among all 20 ×

20 pixels) for which the maximum white pixels are encountered, is located. That radius ***R*** corresponds to the radius of the iris and pixel which was chosen as the center ***C***, which gave that maximum count, is the center of the iris. Although, this method is computationally more expensive then the methods employed in the literature, but, it has been experimentally shown to be far more robust. Therefore this method was employed for all the experimental results (from the CASIA I, CASIA III, and IITD v1 database) reported in this paper.

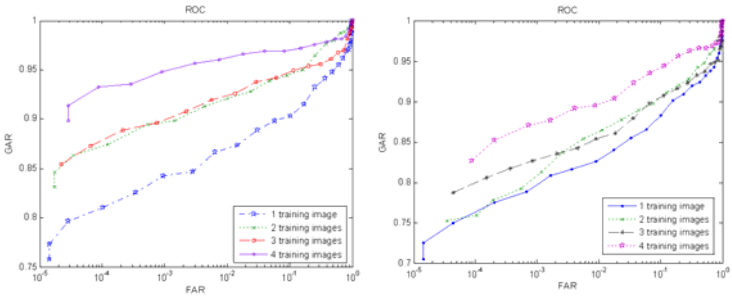

(a) (b)

Figure 4: The ROC from the test data using DCT in (a) and FFT based approach in (b).

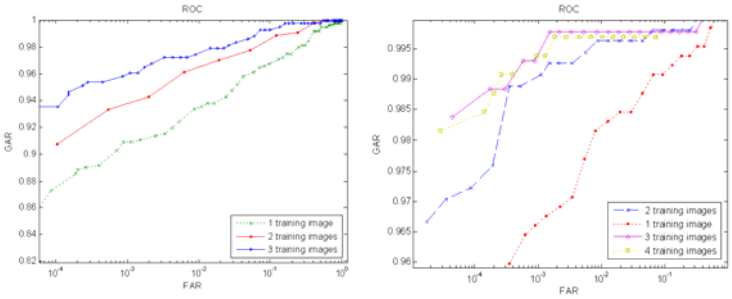

(a) (b)

Figure 5: The ROC from the test data using Haar wavelet in (a) and Log-Gabor filter based approach in (b).

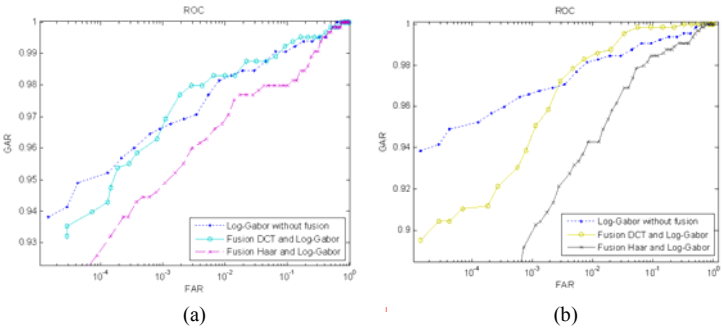

(a) (b)

Figure 6: Fusion of Haar and DCT with Log-Gabor scores using product rule in (a) and min rule in (b).

4. Experiments and Results

The rigorous experiments were performed to select the parameters that can achieve best possible results. The experimental results reported in this paper are in fact the product of our efforts that were focussed to develop a more reliable, low-cost, and online personal identification system at IIT Delhi. We firstly report the experimental results from the four matchers employed to ascertain the performance from the CASIA I and CASIA III iris database which is followed by results from the IITD v1 iris image database [14]. The performance from the four considered matchers significantly varies with the increase in number of training images. Therefore the experiments were performed to ascertain the performance improvement with varying number of training images.

The figure 4(a) illustrates the ROC from the DCT based approach detailed in section 2.1. Similarly, figure 4(b) illustrates the ROC from the FFT based approach as detailed in section 2.2. Significant increase in the performance can be observed with the increase in number of training images while the DCT based approach achieves much better performance as compared to the approach using FFT features. The figure 5 illustrates individual performance from the Haar wavelet and Log-Gabor filter approach.

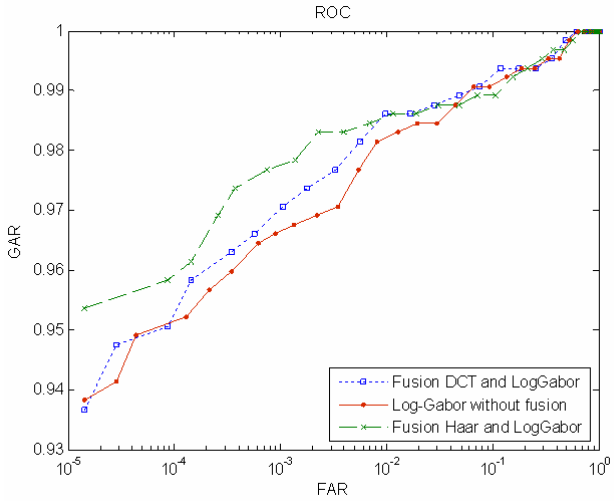

Figure 7: The ROC using weighted sum rule combination from the DCT, Haar and Log-Gabor scores.

The performance from the Log-Gabor filter shown in figure 5(b) is observed to be the best among all the four considered approaches, however its performance does not improve as the number of training images are increased from three to four. This is possiblt due to the overtraining from the increase in number of training images. The performance from the FFT based approach has been the worst among the four considered approaches and therefore this approach was not considered for the score level fusion.

We performed rigorous experiments for the score level combination of best performing three approaches using fixed combination rules. The experimental results from the score level combination using only one/first training image are illustrated in figure 6 and 7. The figure 6 suggests that the performance from the product and min rule has not been

effective in improving the performance. However, the weighted sum rule is quite effective in achieving the performance improvement as can be observed from results in figure 7. The performance improvement from the Haar wavelet and the Log-Gabor filter is significantly higher than those from the DCT and the Log-Gabor filter. Furthermore the Haar wavelt approach requires least amount of computations among all approaches and can be implemented with simple integer processing. Therefore this combination is the most promising to achieve the performance improvement and was further investigated. The equal error rate (EER) and the decidability index (DI) were used to as the quantitative performance indices to ascertain the performance [12]. Table 1 presents the summary of these performance indices on the CASIA I database.

Table 1: Performance Indices from the experiments using CASIA I database.

	One Training		Two Training	
	EER	*DI*	*EER*	*DI*
Log Gabor Filter	1.62	5.4808	0.55	6.4463
Haar Wavelet	4.43	4.6679	2.96	5.3318
Fusion	0.94	5.6948	0.36	6.7175

Table 2: Performance Indices from the experiments using CASIA III database.

	EER	*DI*
Log Gabor Filter	3.72	4.7543
Haar Wavelet	13.16	2.8078
Fusion	2.40	4.6993

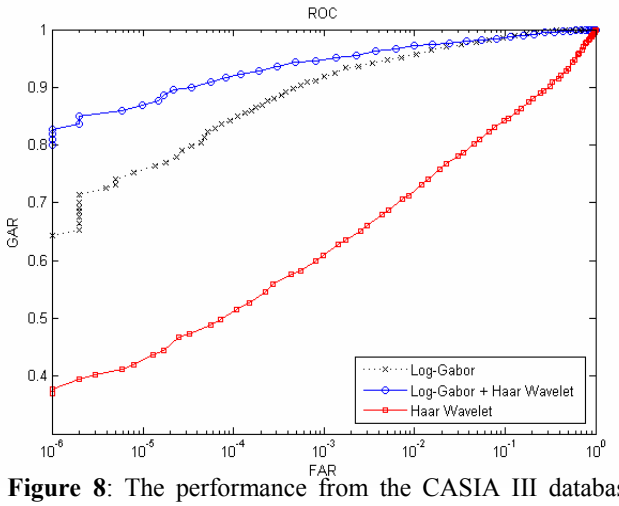

Figure 8: The performance from the CASIA III database (411 users) using only one training image.

The CASIA III [14] iris database with 2877 images, first seven[‡] left iris images, from all 411 users was employed to ascertain the performance. The experimental results from the CASIA III database are summarized in table 2 and also shown in figure 8. These experimental results from the CASIA III database, from all 411 users, involved over 12 million (12 × 1,011,060) comparisons. It can be ascertained from the ROC in figure 8 that the performance improvement, due to the simultaneous usage of Haar wavelet features, is significant. In addition, the IIT Delhi iris database [15] of 1120 images from 224 users was also buildup as our

[‡] Only first seven images were employed to simply to limit the computations involved in generating imposter scores.

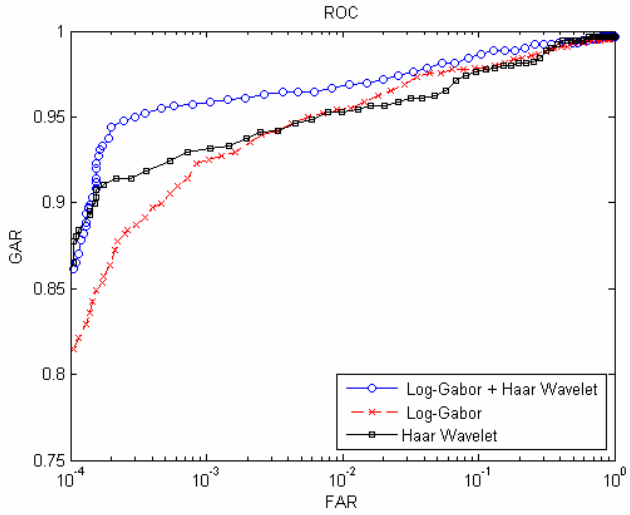

Figure 9: The performance from the IITD database using only one/first training image.

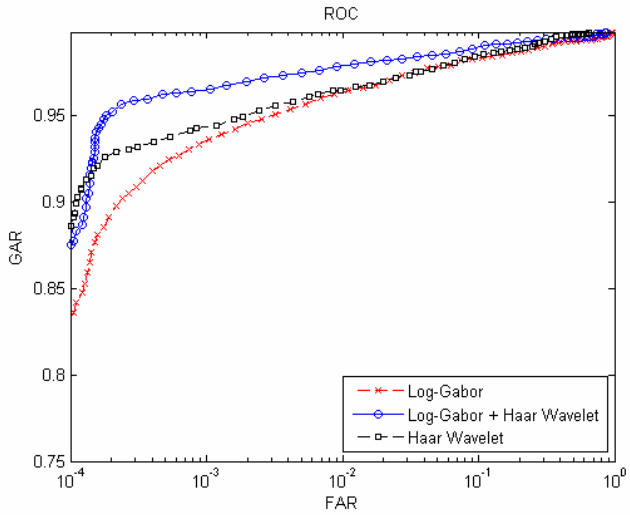

Figure 10: The average performance from the IITD database using only one training image.

Table 3: Performance Indices from the average experiments IITD and CASIA I database.

	IITD		CASIA	
	EER	*DI*	*EER*	*DI*
Log Gabor Filter	2.81	5.7437	2.21	5.2884
Haar Wavelet	3.40	6.1762	3.91	4.8016
Fusion	2.59	6.4079	1.48	5.6640

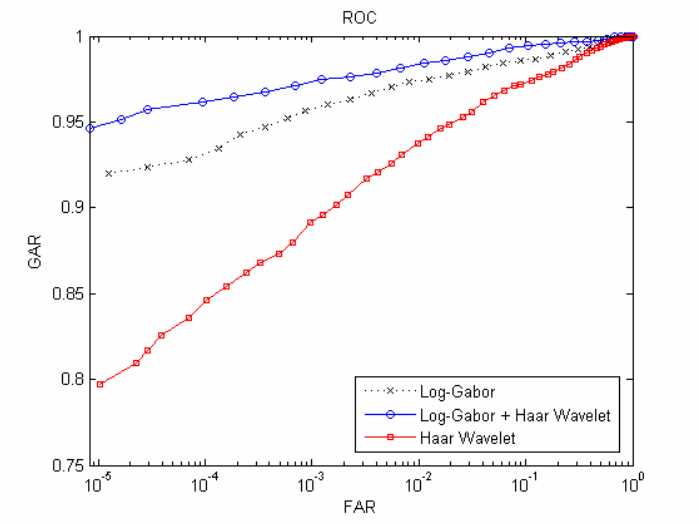

Figure 11: The average performance from the CASIA I database using only one training image.

implementation is completely online and employed *JIRIS JPC1000* iris camera [18]. This database is freely available for the researcher's and was also used to ascertain the performance improvement. The methods for the performance evaluation on IIT Delhi database were same as used for the CASIA database. The performance from the IITD database using the one/first training image is presented in figure 9. The results illustrate the performance improvement due to the simultaneous usage of Haar wavelet features. In order to ascertain the performance improvement from minimum training image, independent of the training image, rigorous experiments were performed to ascertain

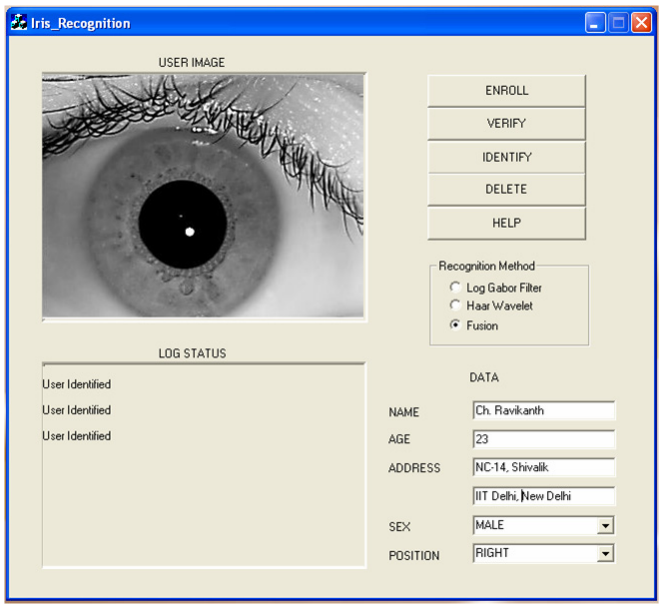

Figure 12: The graphical user interface for developed system

the average performance. In these set of experiments average of results obtained when each of the eight (five for IITD database) images were employed for training and rest of the images as the test set. The average performance from the IITD database and CASIA I database is summarized in the table 3. The corresponding ROCs are illustrated in figure 10 and 11. The performance indices in table 3 suggest that the achieved performance improvement is quite independent of selected training image. The proposed system is implemented in Visual C++ 6.0 on Windows OS environment and figure 12 illustrates the graphical user interface for its online usage. The implemented system can automatically acquire the iris image whenever an eye comes in front of the camera (about 20 centimeters). The CMOS iris camera employed in our standalone implementation is portable (weights 80 grams) and not very expensive (available for 370 US$). The developed system is able to authenticate the individuals in less than a second, using the combination of two approaches, and is tailored for the online usage. The user identification information acquired during the registration is stored in the *MySQL* database.

5. Conclusions

This paper has investigated the comparative performance from four different approaches for the iris identification: DCT, FFT, Haar wavelet and Log-Gabor filter. Our experimental results presented in previous section suggest that the performance from the performance from the Log-Gabor filter is the best which is followed by the Haar wavelet, DCT and FFT in order. This work has also investigated the possible performance improvement using score-level combination. The experimental results suggest that the combination of Log-Gabor and Haar wavelt matching scores using weighted sum rule is the most promising. The extensive evaluation of the proposed combination on CASIA I (108 users), CASIA III (411 users) and IITD (224 users) database achieved significant improvement in the performance. The summary of prior work presented in section 1.2 has suggested that prior efforts have been employing several training images for the performance evaluation. However, the performance evaluation presented in this paper has been focused on the usage of one training image.

The recent comments [16] on CASIA version 1 database illustrates that images in this dataset have their pupil regions masked to suppress the specular reflections from the near IR illuminators. However, such reflections have been easily removed in the pre-processing stage (median filter in figure 3). These reflections are common in CASIA III and IIT Delhi database and thus our implementation does not have any problem in handling pupils with such specular reflections. Therefore we also investigated on CASIA I database, as this database has been extensively used in several of prior publications, and

achieved similar or better performance improvement. The motivation for considering only fixed combination rules in this paper was the fact that this approach does not require any training and is computationally simpler. However, the trainable fusion strategies may offer better performance improvement and is suggested for the investigation in the future efforts.

6. Acknowledgements

This work is partially supported by the research grant from Ministry of Information and Communication Technology, Government of India, grant no. 12(54)/2006-ESD. We thankfully acknowledge the Chinese Academy of Sciences, Institute of Automation, for providing us the CASIA Iris Image Database.

7. References

[1] J. Thornton, M. Savvides, and B. V. K. Vijay Kumar, "A Bayesian approach to deformed pattern matching of iris images," *IEEE Trans. Patt. Anal. Machine Intell.*, vol. 29, pp. 596-606, Apr. 2007.

[2] J. Daugman, "High confidence visaual recognition of persons by a test of statistical independence," *IEEE Trans. Patt. Anal. Machine Intell*., vol. 15, pp. 1148-1161, Nov. 1993.

[3] D. M. Monro, S. Rakshit, and D. Zhang, "DCT-based iris recognition," *IEEE Trans. Patt. Anal. Machine Intell* , vol. 29, pp. 586-595, Apr. 2007.

[4] L. Ma, T. Tan, Y. Wang, and D. Zhang, "Personal identification based on iris texture analysis," *IEEE Trans. Patt. Anal. Machine Intell.*, vol. 25, pp. 1519-1533, 2003.

[5] W. W. Boles, "A security system based on human iris identification using wavelet transform," *Proc. Intl. Conf. Knowledge-Based Intelligent Electronic Systems*, pp. 533-541, May 1997.

[6] L. Ma, T. Tan, Y. Wang and D. Zhang. "Efficient Iris Recognition by characterizing Key Local Variations", *IEEE Trans. Image Process.*, vol. 13, pp. 739-750, 2004.

[7] R.P. Wildes, "Iris Recognition: An Emerging Biometric Technology", *Proc. IEEE*, vol. 85, pp. 1348-1363, 1997.

[8] H. Proença and L. A. Alexandre, "Towards noncooperative iris recognition: A classification approach using multiple signatures," *IEEE Trans. Patt. Anal. Machine Intell.*, vol. 29, pp. 607-612, Apr. 2007.

[9] L. Flom and A. Safir, "Iris Recognition System," *US Patent No*. 4 641 394, 1987.

[10] J. Huang, T. Tan, L. Ma, Y. Wang, "Phase correlation based iris image registration model," *Computer Science and Technology*, vol. 20, no. 3, pp. 419-425, May 2005.

[11] C. H. Daouk, L.A. Esber, F. O. Kanmoun, and M. A. Alaoui. "Iris Recognition", *Proc. ISSPIT*, pp. 558-562, 2002.

[12] L. Masek, *Recognition of human iris pattern for biometric identification*, B. Eng. Thesis, University of Western Australia, 2003. http://www.csse.uwa.edu.au/~pk/studentprojects/libor/index.html

[13] P. Yao, J. Li, X. Ye, Z. Zhuang and B. Li, "Iris Recognition using modified Log-Gabor filters," *Proc. ICPR 2006*, Hong Kong, pp. 1-4, Aug. 2006.

[14] CASIA IRIS Database, http://www.cbsr.ia.ac.in/IrisDatabase.htm

[15] IIT Delhi Iris Database version 1.0, http://web.iitd.ac.in/~biometrics/Database_Iris.htm

[16] P. J. Phillips, K. W. Bowyer and P. J. Flynn, "Comments on the CASIA version 1.0 iris dataset," *IEEE Trans. Patt. Anal. Machine Intell.*, vol. 29, pp. 1869-1870, Oct. 2007.

[17] K. W. Boyer, K. Hollingsworth, P. J. Flynn, "Image understanding for iris biometrics: a survey," *Computer Vision & Image Understanding*, vol. 110, pp. 281-307, May 2008.

[18] http://www.jiristech.com/english/products/iris.php